ASSESSING MERCURY LANDING SITE PROPERTIES WITH MESSENGER HIGH-RESOLUTION IMAGE DATA. Jason Rabinovitch[1*], Asim Qureshi[1], Joshua Bernstein[1], Rebecca Guerra [1], Benjamin Knobloch[1], Campbell Tedtsen[1] and Paul K. Byrne[2], [1]Stevens Institute of Technology, [2]Washington University in St. Louis, [*]Corresponding Author: jrabinov@stevens.edu

Introduction: Some of the most compelling scientific questions we have for Mercury require in-situ measurements—that is, the acquisition of data from the surface of Mercury [1]. Such measurements include sampling of surface materials, the use of seismic signals to probe the planet's interior, and even to sample water ice and organic lag deposits in permanently shadowed regions at the poles [2].

In addition to the tremendous difficulty in safely landing a payload on the surface of Mercury [2], future in-situ Mercury missions would considerably benefit from knowledge of local surface roughness, slope, and the size distribution of hazards (e.g., rocks) in relation to the clearance and stability configuration of the spacecraft. Unfortunately, the resolution of existing orbital image datasets for Mercury precludes landing site assessments analogous to the proven methods developed for Mars landing site analysis (e.g. [3] and references therein, and [4]). A similar challenge exists for analyzing prospective landing sites at Venus, although recent work has demonstrated possible approaches to planetary landing site characterization for the second planet when there is limited high-resolution surface data available [5].

This study focuses on investigating possible correlations between previously mapped geological units on the surface of Mercury—principally, the two major terrain types on the planet, intercrater plains and smooth plains [e.g., 6]—and crater size–frequency distributions. Although relatively limited image data are available of the Mercury surface at resolutions even approaching those needed to characterize landing site safety, those that are available were acquired during the MESSENGER mission's low-altitude campaign [e.g., 7]. On the basis of those images, we test the hypothesis that crater statistics for those two major terrain types are, at the largest map scales, essentially indistinguishable—such that targeting a landing site on a smooth plains deposit, which might seem at face value to be a more forgiven terrain type on which to land, might not constitute any inherent safety advantage than landing at an intercrater plains site. If so, then the scientific return of a Mercury landed mission need not be limited to a particular terrain type.

Image Processing: In this study, we used images from the MESSENGER narrow-angle Mercury Dual Imaging System MDIS NAC [8]. We specifically focused on those images with resolution <5 m/pixel, incidence angles $<70^0$, and mean pixel intensities >0.01 (to filter out dark images), from which we down-selected ~3,500 possible images to analyze.

Preliminary work focused on developing methods for querying the MDIS dataset and associated metadata. For example, the histogram in Fig. 1 shows how many images are available for a given resolution (horizontal pixel scale, with units of pixels/m). Although Fig. 1 only includes images that have a pixel scale <10 m/pixel (and so only considers MDIS NAC images), we found that there are thousands of images that could be considered in this study.

To balance a focus on images with a relatively high resolution (and therefore a fine horizontal pixel scale) with a requirement to analyze images over a range of latitude and longitude values, we visually quantified where on the surface of Mercury has been imaged at high resolution. In Fig. 2, the location of images that meet the quality specifications described above (including having a resolution of <5 m/pixel) are shown. Latitude values fall within a relatively small range, a function of MESSENGER's high northern periapsis, although there is a sufficiently large variation in longitude so as to offer images that span substantial portions of both smooth plains and intercrater plains units at those latitudes. In Fig. 3, we show a similar visualization based on a 3 m/pixel threshold; although there are still ~2,000 images that meet our criteria, they fall into a much narrower longitude range. Therefore, we have set as our minimum image resolution a requirement of 5 m/pixel for our crater statistics analysis.

Ongoing Work: To date, work has primarily focused on software development for scripts and tools to interact with the MDIS dataset, together with the development of an in-house software for documenting craters in the MDIS NAC dataset (Fig. 4). We have now turned to selecting a subset of the images plotted in Fig. 2 for smooth plains and intercrater plains units, as a basis for our crater size–frequency distribution (CSFD) analysis. By quantifying the spatial density and number of craters within those image subsets, we will test the hypothesis that the CSFD values for both smooth plains and intercrater plains units are statistically indistinguishable.

Acknowledgments: The authors acknowledge the support of the Pinnacle Scholars Program at Stevens Institute of Technology, for supporting undergraduate research during the summer of 2022.

References: [1] National Academies of Sciences, Engineering, and Medicine., (2022), Origins, Worlds, and Life: A Decadal Strategy for Planetary Science and Astrobiology 2023-2032. *The National Academies Press*, [2] Ernst et al., (2022), *The Planetary Science Journal*, Vol 3, No 3., [3] Golombek et al., (2012), *Space Sci Rev*, 170, 641–737, [4] Vasavada et al., (2012), *Space Sci Rev*, 170, 793–835, [5] Rabinovitch, J. and Stack, K. M, (2021) *Icarus*, Vol. 363, 114429 [6] Denevi, et al., (2013), *J. Geophys. Res. Planets*, 118, 891– 90, [7] Chabot, et al., (2016), *Geophys. Res. Lett.*, 43, 9461– 9468, [8] Hawkins et al., (2007) *Space Sci Rev* 131, 247–338

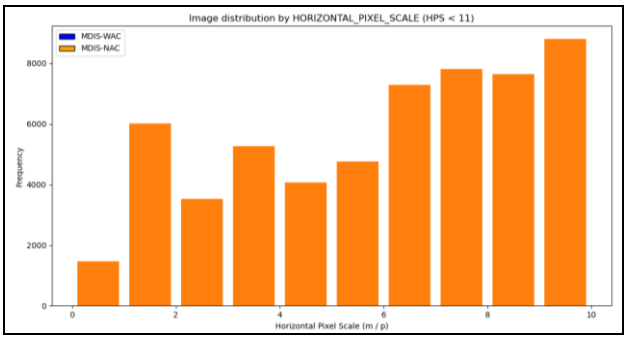

Figure 1. A histogram showing the number of MDIS images available as a function of horizontal pixel scale, for images with a horizontal pixel scale <10 m/pixel.

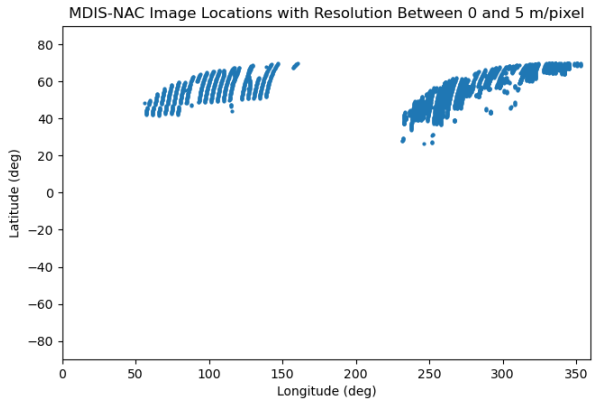

Figure 2. The map locations of MDIS NAC images with a resolution <5 m/pixel, incidence angle < 70^0, mean pixel intensity > 0.01, and an acceptable Data Quality ID, plotted in an equirectangular projection centered at 180°E. We found a total of 3682 images that meet these requirements.

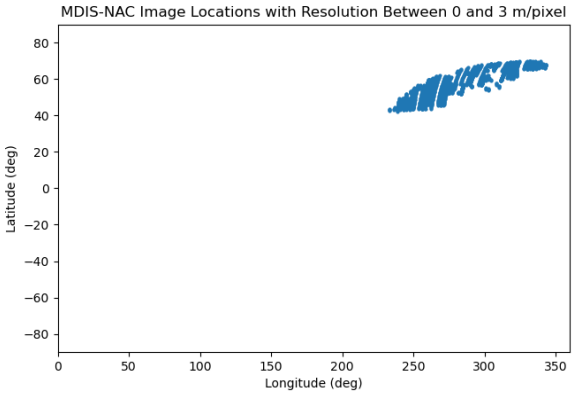

Figure 3. As for Fig. 2, but this time the map locations of MDIS NAC images with a resolution <3 m/pixel (all other criteria held constant). A total of 2221 images meet these requirements.

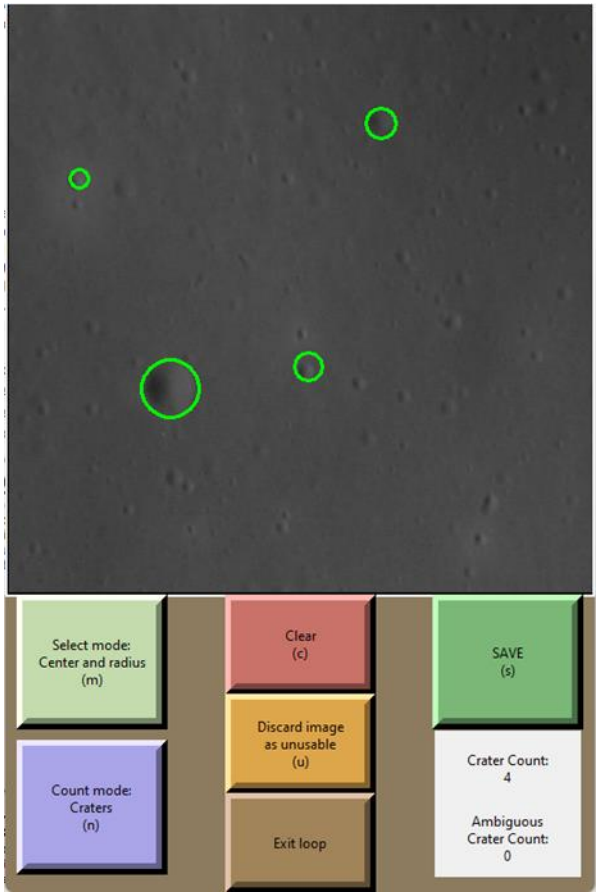

Figure 4 – Sample screenshot from the in-house developed software ("circledrop") that allows a user to specify a specific image in the MDIS-NAC dataset, and then overlay circles on the image that match crater outlines (and save the results for post-processing).